Guest Lecture: Spin-Orbit Resonance and Resonance Capture

Yubo Su

Apr 11, 2024

Note from the author: Hey guys, just wanted to provide a set of reference notes for y'all, since the lecture could have been significantly clearer, and some of these concepts are simple enough that they're worth remembering. I've structured the notes with a general overview section (I swear it's shorter than it looks) with just a few bullet-pointed ideas, and then leave the algebra for the later sections. I hope this helps recapitulate everything we talked about a bit, and I'm sorry for the delay!

1 Overview

In this lecture, we covered three concepts from planetary dynamics: (i) spin-orbit resonance [non-secular], (ii) "secular spin-orbit resonance", and (iii) dissipative resonance capture. A few key ideas to contextualize and summarize our discussion:

- (Non-secular) Spin-Orbit Resonance
  - Key idea: "When the planet is slightly aspherical and elongated, its long axis wants to point towards the host star."
  - Developed mathematically, this long axis oscillates much like a pendulum, with the lowest energy state being permanent alignment along the star-planet axis (pendulum pointing down). This is the 1:1 spin-orbit resonance, where the spin frequency Ω_s of the planet equals its mean motion n (orbital frequency).
  - This can be generalized to eccentric orbits, and pendulum-like equilibria/resonances occur when $\Omega_s/n = k/2$, for integer k.

    This is the cause of Mercury's famous 3:2 spin orbit resonance, where it rotates three times for every two orbits around the Sun: Mercury is eccentric and has a long axis (in the equatorial plane) that tries to point towards the host star.
- Secular Spin-Orbit Resonance
  - Key idea: "When a planet has an equatorial bulge and also has a misaligned companion planet, its spin axis wants to remain in the plane of the two planets' orbit normals."
  - Recall that, in the *secular approximation*, we aim to study long-term behavior of planetary dynamics by averaging over the spin and orbital phases of the planet.
  - In this approximation, a rotating planet (which will exhibit an equatorial bulge) orbiting its host star will experience *spin precession*.

    Because the star gravitationally tugs on the equatorial bulge, this results in a torque that causes the spin vector to "precess" about the planet's orbit normal.

- At the same time, if the planet has a distant, massive companion planet with a misaligned orbit (the orbits are not coplanar), then the planet will undergo *orbital precession*.

  This is because the "ring of mass" (orbit averaged) of the outer companion tugs on the "ring of mass" of the inner planet, causing the orbit normal of the inner planet to precess about that of the outer planet (to be precise, they precess about the axis of their combined angular momentum).
- If the system configuration is such that these two precession frequencies match, then the planet's spin, planet's orbit, and companion's orbit will precess such that they remain in the same plane (alternatively, the planet's spin is fixed in the frame co-precessing with the orbit precession).

  Such configurations are called *Cassini States*.
- For certain ratios of precession frequencies, one of the Cassini States is surrounded by a pendulum-like region of phase space, hence "secular spin-orbit resonance."

- Resonance Capture
  - Resonance capture refers to the process by which a system transitions from circulation (a pendulum swinging [counter]clockwise) to libration within a resonance (a pendulum oscillating about a downwards orientation).
  - The old theory (an earlier lecture in the class) suggests that resonance capture is a process that can be understood for Hamiltonian systems that are varied adiabatically (e.g. a pendulum whose length is slowly changed).
  - Through a careful analysis of critical orbits, we show that resonance capture can also be understood for near-Hamiltonian systems that are Hamiltonian except for a small perturbation (e.g. a pendulum with air resistance; spin-orbit resonance with tidal obliquity damping).

2 The Story

No, this is not "the story" that I told in class, which I remain grateful for everybody's laughter.

Consider a planet with mass $M \gtrsim$ that of the Earth and radius R in orbit around a star with $M_\star = M_\odot$ on a circular orbit with semimajor axis $a \lesssim 1\,\mathrm{AU}$. At such separations, the planet will evolve towards a tidally locked state (spin frequency = orbital frequency, spin axis aligned with orbit normal) on timescales $\lesssim$ Gyr, less than the age of most observed planetary systems.

Suppose that exterior to this planet, a Jupiter-like planet ($M_\mathrm{p} \sim M_\mathrm{Jup}$ at $a_\mathrm{p} \sim 5\,\mathrm{AU}$) is on an orbit inclined to the inner planet's orbit by the mutual inclination I.

We expect that planets may form with large "obliquities", the angle between the planet's spin and orbital axes. As tides act to damp the large primordial obliquity of the inner planet, its obliquity sometimes is trapped at $\sim 90^\circ$. In this lecture, we will explore this process a bit.

The first section, on non-secular spin-orbit resonances, is not relevant for this story, but is included for historical completeness, since it is important in the solar system and is a little more intuitive.

3 Non-Secular Spin-Orbit Resonances

The physical idea here is clear: an elongated planet wants to point its long axis towards its host star (see left hand side of Fig. 1). Conceivably, this is similar to a pendulum, which wants to point

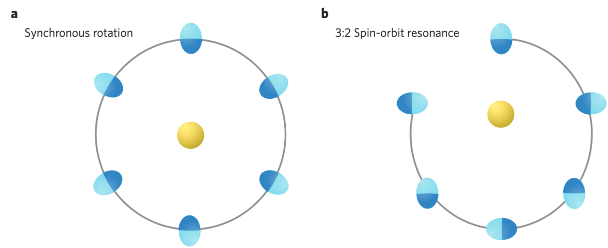

Figure 1: (left) 1:1 spin orbit resonance. (right) Mercury's spin-orbit resonant state [2].

downwards. How can we show this mathematically?

Before we start, note that this is traditionally what people mean when they talk about spin-orbit resonance, since it's literally a commensurability of the spin and orbital frequencies. In exoplanetary dynamics, we've only recently started being able to put direct observational constraints on planetary spin phase, so we typically study secular spin-orbit resonances, described in the next section, and will involve a commensurability of the spin and orbital secular *precession* frequencies instead.

We start by writing down the Hamiltonian governing the spin evolution of the planet. This consists of its rotational kinetic energy as well as the gravitational potential energy of the body, which is the quadrupolar tidal potential to leading order. The potential energy is given by *MacCullagh's Formula* (Tremaine Eq. 1.129 & 7.25), and we arrive at:

$$H_{\rm spin} = \frac{1}{2}\left(\vec{\Omega}_{\rm s} \cdot \mathbf{I} \cdot \vec{\Omega}_{\rm s} + 3\frac{GM_\star}{r^3}\hat{r} \cdot \mathbf{I} \cdot \hat{r} - \frac{GM_\star}{r^3}\,\mathrm{Tr}(\mathbf{I})\right). \tag{1}$$

Here, $\vec{\Omega}_{\rm s}$ is the spin vector of the planet, $M_\star$ is the mass of the host star, r is the distance from the planet to the host star, $\hat{r}$ is the separation direction from the host star, and

$$\mathbf{I} = \int \vec{R}\vec{R}\,\mathrm{d}m = \begin{pmatrix} A & 0 & 0 \\ 0 & B & 0 \\ 0 & 0 & C \end{pmatrix}_{\hat{\imath}\hat{\jmath}\hat{k}}, \tag{2}$$

is the planet's moment of inertia matrix ($\vec{R}$ labels position inside the planet), and we've written its components in its principal axis basis. Here, $A \le B \le C$, and C is the moment of inertia about $\hat{k}$, the shortest principal axis and the one with the largest moment of inertia.

Note that the last term of Eq. (1) does not affect the spin dynamics, as it is spherically symmetric, and only modifies the radial motion of the planet; thus we can ignore it going forward.

3.1 Circular

For simplicity, let's assume the planet's orbit is circular and its spin is along $\hat{k}$ and is aligned with the orbit normal (zero "obliquity", so $\hat{r} \cdot \hat{k} = 0$), i.e. the planet's equator lies in its orbital plane. Then Eq. (1) simplifies to

$$H_{\rm spin} = \frac{C\Omega_{\rm s}^2}{2} + \frac{3n^2}{2}\left[A(\hat{r} \cdot \hat{\imath})^2 + B(\hat{r} \cdot \hat{\imath})^2\right], \tag{3}$$

where $n^2 = GM_\star/a^3$ is the mean motion / orbital angular frequency. But of course, $(\hat{r} \cdot \hat{\imath})^2 = 1 - (\hat{r} \cdot \hat{\imath})^2$, so we can rewrite, dropping another overall constant

$$H_{\rm spin} = \frac{C\Omega_{\rm s}^2}{2} + \frac{3n^2(B-A)}{2}(\hat{r} \cdot \hat{\imath})^2. \tag{4}$$

Now, if $f = nt$ is the planet's true anomaly (uniformly advances at rate n), and ϕ is the spin phase of the planet ($\dot{\phi} = \Omega_{\rm s}$), then (again, subtracting out a constant)

$$H_{\rm spin} = \frac{C\Omega_{\rm s}^2}{2} - \frac{3n^2(B-A)}{4}\cos 2\left(\phi - nt\right). \tag{5}$$

It is quite clear that $H\left(\Omega_{\rm s}, \phi - nt\right)$ looks almost like a pendulum ($H \sim \dot{\theta}^2/2 - \cos\theta$) except that there are two stable equilibria, $\phi = nt$ and $\phi = nt + \pi$. This has a simple interpretation: a planet doesn't care whether its $\hat{\imath}$ axis is aligned or antialigned with $\hat{r}$, the potential will be the same.

3.2 Eccentric

See Murray & Dermott §5.4 or Tremaine §7.2 for a more careful derivation; we will just try to identify the key intuition behind the claim "spin-orbit resonances exist at half-integer ratios of $\Omega_{\rm s}/n$."

The above procedure can be easily generalized to handle an eccentric planet, though we will focus on the zero-obliquity case again for now. We return to Eq. (1) and obtain instead a slightly modified version of Eq. (3):

$$H_{\rm spin} = \frac{C\Omega_{\rm s}^2}{2} + \frac{3GM_\star(B-A)}{2r^3}\left(\hat{r}\cdot\hat{\imath}\right)^2. \tag{6}$$

In an eccentric orbit, $\hat{r}$ no longer advances uniformly with time. Instead, the components in the inertial frame $\hat{r}_x = \cos f$ and $\hat{r}_y = \sin f$ can be expressed as a Fourier series in the *mean anomaly* $\mathcal{M} = nt$, which does advance uniformly (e.g. Murray & Dermott Eqs. 2.84–2.85). This result is quite messy, but broadly speaking:

$$\hat{r} = \left[\sum_{p=0}^\infty P_p \cos k\mathcal{M}\right]\hat{x} + \left[\sum_{q=1}^\infty Q_q \sin q\mathcal{M}\right]\hat{y}, \tag{7}$$

$$\hat{\imath} = \cos\phi\hat{x} + \sin\phi\hat{y}, \tag{8}$$

$$\begin{aligned} H_{\rm spin} &= \frac{C\Omega_{\rm s}^2}{2} + \frac{3GM_\star(B-A)}{2r^3}\left(\hat{r}\cdot\hat{\imath}\right)^2 \\ &= \frac{C\Omega_{\rm s}^2}{2} + \frac{3GM_\star(B-A)}{2r^3} \times \left[(\ldots) - \sum_{p=0}^\infty\sum_{q=1}^\infty F_{pq}\cos\left((p+q)\mathcal{M} - 2\phi\right) + G_{pq}\cos\left((p+q)\mathcal{M} + 2\phi\right)\right]. \end{aligned} \tag{9}$$

The terms are a bit laborious to evaluate out by hand, but the principle of it is clear: we dot the x, y components of $\hat{r}$ and $\hat{\imath}$, then product-to-sum identities give us some coefficient F_{pq} (which depends on the Fourier coefficients P_p and Q_q) multiplied by cosines with the correct arguments, plus a bunch of extra terms (denoted with the "...") that do not have the correct trig argument.

This may look complicated, but the upshot is this: the potential energy term in $H_{\rm spin}$ has a bunch of pendulum-like terms. Each of these angles can "librate" (like pendulum pointing down, where its phase will oscillate about the downward-pointing value), and if so, the system is trapped in this resonance. The set of possible resonant angles is $(p+q)\mathcal{M} \pm 2\phi$ (this angle is called 2γ in Murray & Dermott) for $p \geq 0$ and $q \geq 1$, so librating resonant angles can appear when

$$kn = 2\Omega_{\rm s}, \tag{10}$$

for integer k. This is as expected. **In these resonances, the planet's long axis should point at the host star at pericenter**, also as expected. For $k = 3$, this yields the essence of Mercury's 3:2 spin-orbit resonance (see Fig. 1).

NB: The standard formulation just directly presents the coefficients for different values of k above, e.g. see Murray & Dermott (5.73–5.82) or Tremaine (7.32). For practical use, that is much more direct and suffices, but it's useful to convince ourselves where the coefficients come from.

4 Secular Spin-Orbit Resonance

The physical idea here is a little less obvious, but can be concisely stated: In a 2-planet system where the planetary orbits are not coplanar, and if a planet's obliquity (denoted $\theta \equiv \arccos \hat{\Omega}_{\rm s} \cdot \hat{l}$) is at the right value, then the planet's spin will tend to want to align with the plane containing the two planets' orbit normals. This effect happens due to *secular* precession frequencies, dynamics arising after averaging over the spin and orbits of the planets.

Note that most of this disussion follows Su and Lai [9], which is a very physically motivated discussion of "Colombo's Top", the simplest model for secular spin-orbit resonance. This is an old system though, dating back to Colombo [1], Henrard and Murigande [7] as some classic references that approach this from a very celestial-mechanics point of view. Scott Tremaine's textbook also covers this in Chapter 7.

For simplicity, we will assume that all orbits are circular, though the derivations are not too significantly altered if the orbits are eccentric.

4.1 Precession Equations

First, we need to briefly discuss our planetary model. Most commonly, a planet is modeled as a self-gravitating, rotating fluid. Thus, the fluid satisfies hydrostatic equilibrium, including the centrifugal potential, and will bulge slightly at the equator. This has two ramifications for spin dynamics: (i) $A = B < C$, where $A = B$ because the planet is axially symmetric about its short polar axis $\hat{k}$ (we call this "oblate"); and (ii) $\hat{\Omega}_{\rm s} = \hat{k}$, i.e. the planet spins about its polar axis[1]. In particular, because the centrifugal potential $\propto \Omega_{\rm s}^2$, it is a textbook exercise to show that

$$\frac{C - A}{MR^2} \propto \Omega_{\rm s}^2. \tag{11}$$

To be more precise, the often used relationship is

$$J_2 \equiv \frac{C - A}{MR^2} = \frac{k_2}{3} \frac{\Omega_{\rm s}^2}{GM/R^3}, \tag{12}$$

where k_2 is the "second Love number" (an order-unity number quantifying how centrally concentrated a body's mass is—for a body of uniform density, $k_2 = 1.5$, while for planets it is typically ~ 0.5–1) and M and R are the planet's mass and radius. This scaling makes sense: if the rotation rate is of order the dynamical infall rate $\sqrt{GM/R^3}$, then the planet's rotational flattening is of order unity.

How does this lead to spin precession? Well, the gravitational potential component of the spin Hamiltonian for an oblate planet (no longer assuming zero obliquity) reads:

$$\begin{aligned} V_{\rm spin} &= \frac{3n^2}{2} \hat{r} \cdot \mathbf{I} \cdot \hat{r} \\ &= \frac{3n^2}{2} \left[r_i^2 A + r_j^2 B + r_k^2 C \right], \end{aligned} \tag{13}$$

where $r_i \equiv \hat{r} \cdot \hat{\imath}$ etc. (I'll try to refrain from using this shorthand for the most part). Then, since $B = A$, and $r_i^2 + r_j^2 + r_k^2 = 1$, we can subtract out a constant to obtain

$$V_{\rm spin} = \frac{3n^2(C - A)}{2} \left(\hat{r} \cdot \hat{k} \right)^2. \tag{14}$$

[1]Fun dynamics occur when considering the spin evolution of satellites or rocky planets, see Gladman et al. [4] or a submitted paper by Yuan, Su, & Goodman 2024.

Next, we want to get from this potential to spin precession, for which there are multiple methods, see Tremaine §7.1 for an alternative option. Here's a coarse idea. Now, if the planet has zero obliquity, then $\hat{r}$ (in the orbital plane) also lies along the equator of the planet, and $\hat{r}\cdot\hat{k}=0$, while if the planet's obliquity is exactly 90°, then $\hat{r}\cdot\hat{k}$ varies sinusoidally between $[-1,1]$, and its square time-averages to 1/2. Thus, it's an easy guess (and can be verified; Tremaine Eq. 7.3) that

$$\langle V_{\rm spin}\rangle = \frac{3n^2(C-A)}{4}\left(\hat{l}\cdot\hat{k}\right)^2 = \frac{3n^2(C-A)}{4}\left(\hat{l}\cdot\hat{\Omega}_{\rm s}\right)^2, \tag{15}$$

where I've replaced $\hat{k}=\hat{\Omega}_{\rm s}$. I'll drop the angle brackets, which denote secular averaging, going forwards.

To understand the evolution of the spin axis, we apply the following:

$$\frac{{\rm d}\hat{\Omega}_{\rm s}}{{\rm d}t} = -\frac{1}{S}\nabla_{\hat{\Omega}_{\rm s}} V_{\rm spin}, \tag{16}$$

where $S\equiv C\Omega_{\rm s}$ is the magnitude of the spin angular momentum. This has many interpretations, all of which analyze the torque the point-mass host star experiences, two of which are: it's a torque on the host star (Tremaine 7.2), or it's an application of the Milankovich Equations (but for a circular orbit).

Somewhat laboriously, we've arrived at one of the results from Su and Lai [9], Eq. (1):

$$\frac{{\rm d}\hat{\Omega}_{\rm s}}{{\rm d}t} = \omega_{\rm sl}\left(\hat{\Omega}_{\rm s}\cdot\hat{l}\right)\left(\hat{\Omega}_{\rm s}\times\hat{l}\right), \tag{17}$$

$$\omega_{\rm sl}\equiv\alpha = \frac{3n^2(C-A)}{2C\Omega_{\rm s}}. \tag{18}$$

This spin precession frequency is commonly denoted α in the literature.

I'll not belabor the orbital precession: two mutually inclined planets will experience orbital precession about their combined angular momentum axis (secular Laplace-Lagrange theory, which was covered earlier in the course; Tremaine S5.2). If the outer planet has much more angular momentum than the inner planet (as in our canonical story), then the dynamics can be approximated as precession of the inner planet $\hat{l}$ about the perturbing outer planet $\hat{l}_{\rm p}$:

$$\frac{{\rm d}\hat{l}}{{\rm d}t} = \omega_{\rm lp}\left(\hat{l}\cdot\hat{l}_{\rm p}\right)\left(\hat{l}\times\hat{l}_{\rm p}\right) \equiv -g\left(\hat{l}\times\hat{l}_{\rm p}\right), \tag{19}$$

$$\omega_{\rm lp}\equiv -\frac{g}{\cos I} = \frac{3M_{\rm p}}{4M_\star}\left(\frac{a}{a_{\rm p}}\right)^3 n. \tag{20}$$

The precession frequency $g<0$ is often defined for reasons unclear to me.

Eqs. (17–19) describe the mutual motion of the two vectors $\hat{\Omega}_{\rm s}$ and $\hat{l}$ with reference to the fixed vector $\hat{l}_{\rm p}$.

4.2 Secular Spin-Orbit Resonance: Cassini States

One nice insight is that, since $\hat{l}$ precesses uniformly about $\hat{l}_{\rm p}$, we can perform a change of reference frame to co-precess with $\hat{l}$ about $\hat{l}_{\rm p}$:

$$\left(\frac{{\rm d}\hat{l}}{{\rm d}t}\right)_{\rm rot} = 0, \tag{21}$$

$$\left(\frac{{\rm d}\hat{\Omega}_{\rm s}}{{\rm d}t}\right)_{\rm rot} = \alpha\left(\hat{\Omega}_{\rm s}\cdot\hat{l}\right)\left(\hat{\Omega}_{\rm s}\times\hat{l}\right) + g\left(\hat{\Omega}_{\rm s}\times\hat{l}_{\rm p}\right). \tag{22}$$

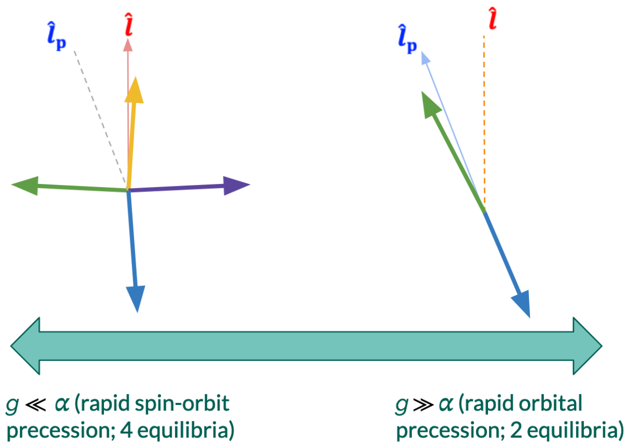

Figure 2: Locations of the Cassini States (spin equilibria) in the two limits $g \ll \alpha$ and $g \gg \alpha$. Note that CS1 and CS2 are stable ("centers" in the dynamical systems language) as long as the tidal dissipation is sufficiently small, but CS3 is only stable if tidal dissipation is exactly zero. CS4 is a saddle point.

In talks, I like to call this trick "I'm a lazy dynamicist, and two moving vectors is one too many."

Cassini States: next, we identify the equilibria of Eq. (22). These spin states are where $\hat{\Omega}_s$ is fixed in the co-precessing frame. In the inertial frame, $\hat{\Omega}_s$ remains in a fixed orientation with $\hat{l}$ and $\hat{l}_p$; as we shall soon see, Cassini States (CSs) for $\hat{\Omega}_s$ are actually coplanaar with the $\hat{l}$–$\hat{l}_p$ plane.

We begin with a simple qualitative analysis, in the two limiting cases where $g \ll \alpha$ and where $g \gg \alpha$, as illustrated in Fig. 2:

- In the former case, spin equilibria occur whenever $\left(\hat{\Omega}_s \cdot \hat{l}\right) = 0$ or when $\left(\hat{\Omega}_s \times \hat{l}\right) = 0$; this implies two CSs with $\hat{\Omega}_s \parallel \hat{l}$ and two with $\hat{\Omega}_s \perp \hat{l}$.

- In the latter case, spin equiibria only occur when $\hat{\Omega}_s \parallel \hat{l}_p$. Thus, there are only two CSs in this limit.

To do this more quantitatively, we adopt a spherical coordinate system in the co-precessing frame such that $\hat{z} = \hat{l}$, $\hat{l}_p \times \hat{l} \propto \hat{y}$, and the spherical coordinates are the polar angle θ and the azimuthal angle ϕ. For convenience going forward, we rescale time such that $\tau = \alpha t$ and

$$\eta \equiv -\frac{g}{\alpha}. \tag{23}$$

Then the equations of motion are

$$\frac{\mathrm{d}\theta}{\mathrm{d}\tau} = \eta \sin I \sin\phi \tag{24}$$

$$\frac{\mathrm{d}\phi}{\mathrm{d}\tau} = -\cos\theta + \eta\left(\cos I + \sin I \cot\theta \cos\phi\right), \tag{25}$$

where $I = \arccos\left(\hat{l} \cdot \hat{l}_p\right)$ is the mutual inclination. The solutions to this system are shown in Fig. 3. It can be shown that the number of CSs changes from 2 to 4 when η crosses the critical value

$$\eta_c \equiv \left(\sin^{2/3} I + \cos^{2/3} I\right)^{-3/2}. \tag{26}$$

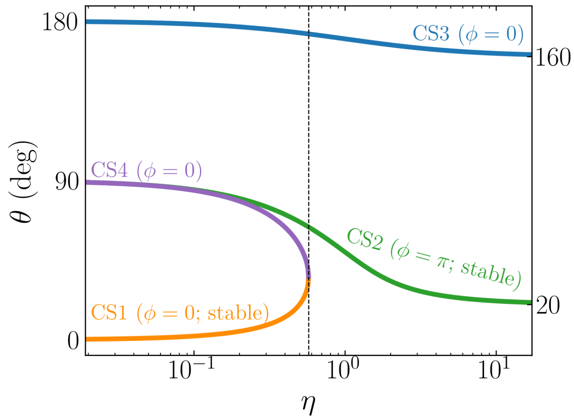

Figure 3: Locations of the Cassini States for $I = 20°$, the equilibria to Eqs. (28–29), where $\eta = -g/\alpha$ (Eq. 23). Note the agreement, in terms of the number of CSs, with Fig. 2. The vertical line is $\eta_{\rm c}$ given by Eq. (26).

Finally, to see the resonant structure of the CS equilibria, it is easiest to directly plot the level curves of the Hamiltonian. In terms of the rescaled coordinates,

$$\begin{aligned} H &= -\frac{1}{2}\left(\hat{\Omega}_{\rm s}\cdot\hat{l}\right)^2 + \eta\left(\hat{\Omega}_{\rm s}\cdot\hat{l}_{\rm p}\right) \\ H(\cos\theta,\phi) &= -\frac{1}{2}\cos^2\theta + \eta\left(\cos\theta\cos I - \sin I\sin\theta\cos\phi\right), \end{aligned} \tag{27}$$

where we've expressed H in terms of the canonically conjugate coordinates $(\cos\theta, \phi)$[2] The level curves for this, in terms of η, are shown in Fig. 4. **Note that when $\eta < \eta_{\rm c}$, and there are four CSs, that the green point ("Cassini State 2") is surrounded by a separatrix, and is reminiscent of a pendulum's phase space.**

5 Tidal Dissipation and Resonance Capture

Key point: Tidal dissipation causes the system to deviate from the perfectly Hamiltonian evolution above. Most interestingly, if the obliquity is initially $> 90°$, then tidal dissipation, as it damps the obliquity towards $0°$, will cause the system to evolve through the separatrix in the top-left panel of Fig. 4. There is then some probability associated with the outcome of this encounter; sometimes, it enters the separatrix, and sometimes it does not. Qualitatively, this can be understood as a small splitting of the separatrix induced by the tidal dissipation, which permits some trajectories to enter the separatrix and rejects others.

Tidal dissipation occurs when the gravitational field of the host star raises a small bulge in the fluid of the planet (like the Sun and moon raise bulges on the Earth's oceans). The bulge both wants to point at the host star and wants to rotate with the planet; these conditions are only in agreement when the planet is *tidally locked*, with zero obliquity and at spin-orbit synchronization. Otherwise, dissipation ensues, where the obliquity will damp to zero and the planet's spin rate will be driven to synchronization. We will focus on just the first effect (obliquity damping) for simplicity and mostly discuss §3 of Su and Lai [9]; see §4 of Su and Lai [9] for the treatment including full tidal dissipation.

[2] That these two are canonically conjugate is not immediately obvious, but when considering the orbit of the Sun in the spin-frame of the planet, the Delaunay variables $G\cos i, \Omega$ are conjugate, which translates to $\cos\theta, \phi$ in the inertial frame when G is constant. Alternatively, this is the condition necessary for Eq. (16) to work.

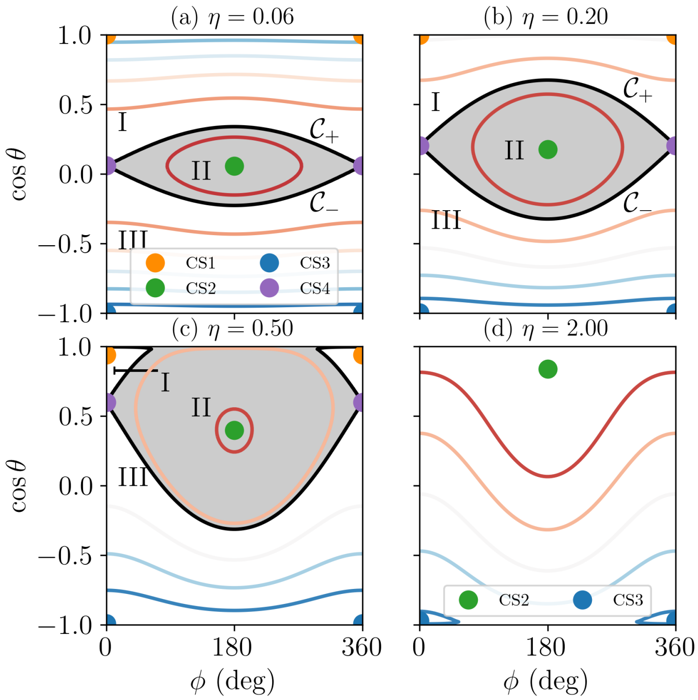

Figure 4: Contour plots of the Cassini State Hamiltonian, Eq. (27), for a few different values of η.

With a slow tidal obliquity damping torque, we can modify the equations in the following prescriptive (read: made-up) way:

$$\frac{\mathrm{d}\theta}{\mathrm{d}\tau} = \eta \sin I \sin\phi - \frac{1}{\tau_{\mathrm{al}}} \sin\theta, \tag{28}$$

$$\frac{\mathrm{d}\phi}{\mathrm{d}\tau} = -\cos\theta + \eta\left(\cos I + \sin I \cot\theta \cos\phi\right), \tag{29}$$

The idea is that tidal dissipation will damp θ on the characteristic rescaled time $\tau_{\mathrm{al}} \gg 1$ (i.e. much slower than all precession frequencies in the system).

For completeness, I must mention: the first way that tidal dissipation affects the Cassini State dynamics is by changing the stability of the Cassini States; see Fabrycky et al. [3] for the most famous discussion of this. In simplest terms, any tidal dissipation turns CS3 from a stable fixed point into a source, while sufficiently strong tidal dissipation does the same to CS2; CS4 remains a saddle point (unstable), and CS1 goes to zero obliquity (the tidally locked state). But that will not be our focus today.

We ask the simple question: for an arbitrary initial condition (θ, ϕ), what is the ultimate fate of the system? This is a very easy question to answer when $\eta > \eta_c$: since only CS2 and CS3 exist (bottom-right panel of Fig. 4), and CS3 is unstable to tidal dissipation, everything ends up at CS2. When $\eta < \eta_c$, two more cases can be solved straightforwardly:

- If the initial condition is in Zone I (labelled on Fig. 4; roughly the set of prograde $\theta < 90°$ initial conditions), then tides will drive the system to CS1, the only stable equilibrium in this region of phase space.

- If the initial condition is in Zone II, tides drives the system to CS2 instead.

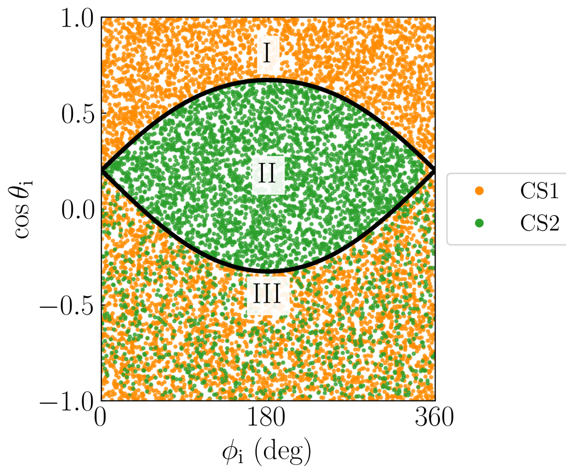

Figure 5: Results of numerical experiments, where each dot is an initial condition that is integrated until it can be identified as reaching CS1 (orange) or CS2 (green). Note the seemingly-probabilistic outcome of trajectories in Zone III.

- **But if the initial condition is in Zone III**, no tidally stable equilibria can be reached without encountering the separatrix. So we must study what happens during this encounter.

This is summarized in Fig. 5.

5.1 Critical Orbits: Graphical Picture

For reference, for this entire section, we keep Fig. 6 on our minds.

Let's imagine the evolution of a significantly retrograde (Zone III) initial condition, as it evolves. For simplicity of discussion, let's assume that the initial condition is at $\phi = 0$ (though of course, for any initial condition, we can just wait a fraction of a precession cycle to reach this):

- Current location: $(\cos\theta_0, 0)$. After a single precession cycle ($\phi = 0 \to \phi = 2\pi$), the system would return to its initial $\cos\theta$ in the absence of tidal dissipation. Including tidal dissipation, $\cos\theta$ increases by a small amount Δ to $\cos\theta_1$.
- Current location: $(\cos\theta_1, 0)$. After a second precession cycle ($\phi = 2\pi \to \phi = 4\pi$), $\cos\theta$ increases by another $\approx \Delta$ to $\cos\theta_2$, now that it is $\approx 2\Delta$ higher than its initial value.
- Current location: $(\cos\theta_2, 0)$.
- ...

  When does this process terminate? When, over the course of a precession cycle, the trajectory encounters the separatrix. Thus, this evolution changes character when:
- Current location: $(\cos\theta_N, 0)$. In the course of the next precession cycle, the trajectory encounters the separatrix.

What must the value of $\cos\theta_N$ be? There are two easy bounds to establish:

- Consider the critical value such that after one precession orbit, it exactly reaches the saddle point; this is denoted by the black circle in Fig. 6. If we are below this value, we will experience one more precession cycle before separatrix encounter; $\cos\theta_N$ must be above the black circle.

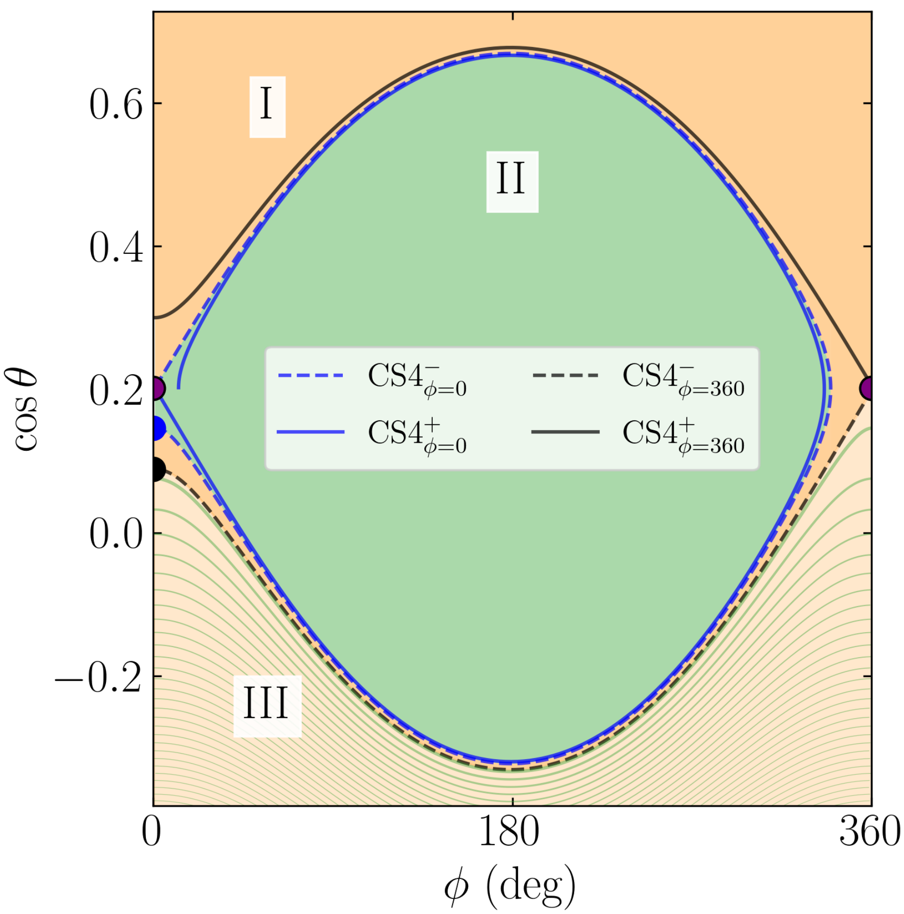

Figure 6: Plot of the critical orbits / manifolds under the effect of tidal dissipation. Orange colored regions will tidally evolve towards CS1, and green regions to CS2. The notation $\mathrm{CS4}^{+}_{\phi=0}$ denotes the orbit starting at CS4 (the saddle point) and $\phi = 0$ evolved forwards in time. Compare to Fig. 5.

- However, $\cos\theta_N$ cannot be above the saddle point, because then on its previous precession cycle, it must have encountered the separatrix. Thus, $\cos\theta_N$ must be below the purple circle in Fig. 6.

We have thus established that, on the separatrix-crossing orbit, the trajectory must start between the black and purple dots in Fig. 6. Determining the outcome of this separatrix crossing orbit requires identifying a second critical orbit. Consider the point obtained by evolving the saddle point backwards in time along the *top* of the separatrix (blue dashed line in Fig. 6), which terminates in the blue dot. At this point, we can just "color in between the lines": points that are connected to the interior of the separatrix can be shaded green, points that are exterior can be shaded orange, and **the outcome of the separatrix-crossing orbit depends on whether $\cos\theta_N$ is above/below the blue dot.**

5.2 Capture Probability: Perturbative Analysis

Above, we have provided the essence of the dissipative capture probability argument. Next, it only remains to calculate the distances between the curves. We can do this with some simple perturbation theory on H, the value of the unperturbed Hamiltonian (which would be conserved in the absence of tidal dissipation). Denoting the top and bottom halves of the separatrix by $\mathscr{C}_\pm$ (see Fig. 4), we can find that

$$H_{\rm purple} = H_{\rm CS4} = H(\cos\theta_{\rm CS4}, 0), \tag{30}$$

$$H_{\rm black} = H_{\rm CS4} - \int\limits_{\mathscr{C}_-} \frac{\mathrm{d}H}{\mathrm{d}t}\,\mathrm{d}t, \tag{31}$$

$$H_{\rm blue} = H_{\rm CS4} - \int\limits_{\mathscr{C}_-} \frac{\mathrm{d}H}{\mathrm{d}t}\,\mathrm{d}t - \int\limits_{\mathscr{C}_+} \frac{\mathrm{d}H}{\mathrm{d}t}\,\mathrm{d}t. \tag{32}$$

Since tidal dissipation is small, all three of these values are very near $H_{\rm CS4}$. Thus, for any initial condition, its specific value of H in the interval $H \in [H_{\rm purple}, H_{\rm black}]$ is nearly uniformly distributed. Thus, the probability of resonance capture into the separatrix is given by the fraction of the interval that is captured:

$$\begin{aligned} P_{\rm cap} &= \frac{H_{\rm purple} - H_{\rm blue}}{H_{\rm purple} - H_{\rm black}}, &(33)\\ &= \frac{\int\limits_{\mathscr{C}_-} \frac{\mathrm{d}H}{\mathrm{d}t}\,\mathrm{d}t + \int\limits_{\mathscr{C}_+} \frac{\mathrm{d}H}{\mathrm{d}t}\,\mathrm{d}t}{\int\limits_{\mathscr{C}_-} \frac{\mathrm{d}H}{\mathrm{d}t}\,\mathrm{d}t}. &(34)\end{aligned}$$

Next, we can identify that

$$\begin{aligned} \int\limits_{\mathscr{C}_\pm} \frac{\mathrm{d}H}{\mathrm{d}t}\,\mathrm{d}t &= \int\limits_{\mathscr{C}_\pm} \frac{\partial H}{\partial\cos\theta}\frac{\mathrm{d}\cos\theta}{\mathrm{d}t} + \frac{\partial H}{\partial\phi}\frac{\mathrm{d}\phi}{\mathrm{d}t}\,\mathrm{d}\phi, &(35)\\ &= \int\limits_{\mathscr{C}_\pm} \left(\frac{\partial\cos\theta}{\partial t}\right)_{\rm tide}\frac{\mathrm{d}\phi}{\mathrm{d}t}\,\mathrm{d}t, &(36)\\ &= \int\limits_{\mathscr{C}_\pm} \left(\frac{\partial\cos\theta}{\partial t}\right)_{\rm tide}\mathrm{d}\phi. &(37)\end{aligned}$$

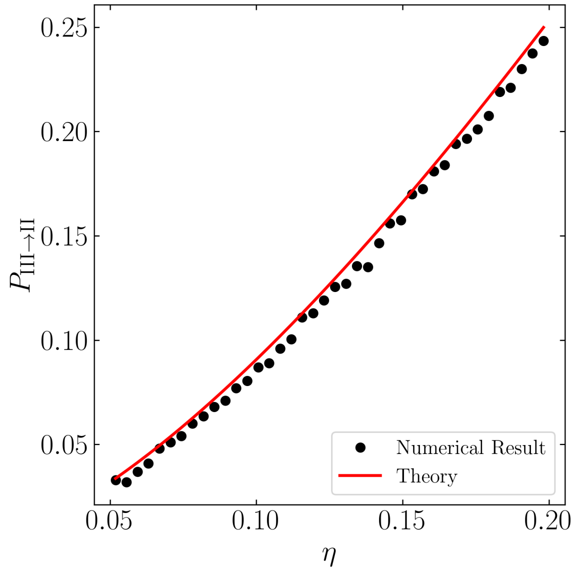

Figure 7: Comparison of the capture probability Eq. (42) compared with numerical experiments.

We next need to evaluate this integral, so we need the curves parameterizing the separatrix, $\mathscr{C}_\pm$. Using Eq. (27) and evaluting at CS4, it is easy to obtain that legs of the separatrix, described by the curve $\cos\theta(\phi)$, is given by

$$(\cos\theta)_{\mathscr{C}_\pm} \approx \eta\cos I \pm \sqrt{2\eta\sin I\left(1-\cos\phi\right)}. \tag{38}$$

Thus, we obtain that (note that $\mathrm{d}\phi$ has different signs along the different legs of the separatrix)

$$\int\limits_{\mathscr{C}_\pm} \frac{\mathrm{d}H}{\mathrm{d}t}\,\mathrm{d}t = \int\limits_{\mathscr{C}_\pm} \frac{1-\cos\theta}{\tau_{\mathrm{al}}}\,\mathrm{d}\phi, \tag{39}$$

$$= \mp\frac{1}{\tau_{\mathrm{al}}}\int\limits_0^{2\pi} 1-2\eta\sin I\left(1-\cos\phi\right) \mp 2\eta\cos I\sqrt{2\eta\sin I}\left(1-\cos\phi\right)\,\mathrm{d}\phi, \tag{40}$$

$$= \mp\frac{1}{\tau_{\mathrm{al}}}\left[2\pi\left(1-2\eta\sin I\right) \mp 2\eta\cos I\sqrt{2\eta\sin I}\left(4\sqrt{2}\right)\right], \tag{41}$$

$$P_{\mathrm{cap}} = \frac{16\eta\cos I\sqrt{\eta\sin I}}{2\pi\left(1-2\eta\sin I\right)}. \tag{42}$$

This works very well, as seen in Fig. 7 of Su and Lai [9] (reproduced here as Fig. 7).

Brief aside, the computation of the distance between these critical orbits is also known in the applied math community as *Melnikov's method* (§4.5 of 5), where it is used to compute the distance between the *stable and unstable manifolds* of the saddle point (what I've called critical orbits above). In astrophysical dynamics, Melnikov's integral is used instead to detect chaos traditionally (§4.3.4 of 8).

5.3 Relation to Adiabatic Resonance Capture

Previously, you learned that when a Hamiltonian system has a parameter that is adiabatically varied (e.g. pendulum with changing length), the probabilities of transitions between two zones i, j of phase space with areas A_i, A_j is given by

$$P_{i\to j} = -\frac{\dot{A}_j}{\dot{A}_i}. \tag{43}$$

This is simple to understand: since the Hamiltonian is varying adiabatically, and phase space volume is an adiabatic invariant (Liouville's Theorem), the probability of this transition occuring just comes down to where the phase space volume lost by zone i is going: how much of it is going to zone j, how much to some other zone k.

Interestingly, this adiabatically varying Hamiltonian formalism and the dissipative formalism I present above can be shown to be equivalent: Henrard [6] gives a way of reducing a dissipative system to a Hamiltonian one (with time dependence)! For the curious ones.

References

[1] Colombo, G. (1966). Cassini's second and third laws. *Astronomical Journal, Vol. 71, p. 891 (1966)*, 71:891.

[2] Ćuk, M. (2012). Kick for the cosmic clockwork. *Nature Geoscience*, 5(1):7–8.

[3] Fabrycky, D. C., Johnson, E. T., and Goodman, J. (2007). Cassini states with dissipation: Why obliquity tides cannot inflate hot jupiters. *The Astrophysical Journal*, 665(1):754.

[4] Gladman, B., Quinn, D. D., Nicholson, P., and Rand, R. (1996). Synchronous locking of tidally evolving satellites. *Icarus*, 122(1):166–192.

[5] Guckenheimer, J. and Holmes, P. (2013). *Nonlinear oscillations, dynamical systems, and bifurcations of vector fields*, volume 42. Springer Science & Business Media.

[6] Henrard, J. (1993). The adiabatic invariant in classical mechanics. In *Dynamics Reported: Expositions in Dynamical Systems*, pages 117–235. Springer.

[7] Henrard, J. and Murigande, C. (1987). Colombo's top. *Celestial mechanics*, 40(3-4):345–366.

[8] Morbidelli, A. (2002). *Modern celestial mechanics : aspects of solar system dynamics*. CRC Press.

[9] Su, Y. and Lai, D. (2022). Dynamics of colombo's top: tidal dissipation and resonance capture, with applications to oblique super-earths, ultra-short-period planets and inspiraling hot jupiters. *Monthly Notices of the Royal Astronomical Society*, 509(3):3301–3320.